# Critical length and dimension elevation

Carolina Vittoria Beccari, Giulio Casciola, Marie-Laurence Mazure

# Critical length and dimension elevation

Carolina Vittoria Beccari[1], Giulio Casciola[1], Marie-Laurence Mazure[2]

[1] *Dipartimento di Matematica, Alma Mater Studiorum Università di Bologna, Piazza di Porta San Donato 5, 40126 Bologna, Italy*
[2] *Université Grenoble Alpes, Laboratoire Jean Kuntzmann, CNRS, UMR 5224, F-38000 Grenoble, France*
carolina.beccari2@unibo.it, giulio.casciola@unibo.it, marie-laurence.mazure@univ-grenoble-alpes.fr

**Keywords:** Extended Chebyshev spaces; critical length (for design); dimension elevation; shape preservation; geometric design.

**AMS subject classification:** 65D17, 65D07

## 1 Introduction

The present report is a useful complement to the short note [4] entitled *"Dimension elevation is not always corner-cutting"* recently submitted for publication.

We work with kernels of linear differential operators with constant real coefficients. Let $\mathcal{L}_n = p_n(D)$ be such an operator of order $(n+1)$, where $D$ stands for the ordinary differentiation and where the associated characteristic polynomial $p_n$ has unit leading coefficient. The $(n+1)$-dimensional space $\mathbb{E}_n := \ker \mathcal{L}_n$ is a *W-space on* $\mathbb{R}$, in the sense that, on the whole of $\mathbb{R}$, no non-zero element of $\mathbb{E}_n$ can have a zero of multiplicity $(n+1)$, or as well, the Wronskian $W(U_0, \ldots, U_n)$ of any basis $(U_0, \ldots, U_n)$ of $\mathbb{E}_n$ does not vanish on $\mathbb{R}$. The space $\mathbb{E}_n$ is closed under translation, and therefore under differentiation. The *critical length* of $\mathbb{E}_n$ is the number $\ell_n \in ]0, +\infty]$ such that $\mathbb{E}_n$ is an *Extended Chebyshev space on [0,h]* (for short, *EC-space on* $[0, h]$) if and only if $h < \ell_n$. That $\mathbb{E}_n$ is an EC-space on $[0, h]$ means that any non-zero element of $\mathbb{E}_n$ has at most $n$ zeros in $[0, h]$, counting the multiplicities up to $(n+1)$. Recall that $\ell_n = +\infty$ if and only $p_n$ has only real roots. If this is not true, the explicit calculation of the critical length $\ell_n < +\infty$ is in general not trivial, unless for specific examples, or very low value of the integer $n$. Fortunately, it can now be determined numerically through the procedure developed in [3]. This numerical test will be essential here.

The space $\mathbb{E}_n$ contains the constants if and only if $p_n(0) = 0$. If so, the $n$-dimensional space $D\mathbb{E}_n$ is in turn the kernel of a linear differential operator with constant coefficients. Its critical length $\widetilde{\ell}_n \leqslant \ell_n$ is called the *critical length for design* of the space $\mathbb{E}_n$. Choose any $h < \widetilde{\ell}_n$. Then $\mathbb{E}_n$ is an EC-space *good for design on* $[0, h]$, *i.e.*, not only it is an EC-space on $[0, h]$, but it even possesses a *Bernstein basis relative to* $(0, h)$, that is, a normalised basis $(B_0, \ldots, B_n)$ such that, for $i = 0, \ldots, n$, first $B_i$ vanishes $i$ times at 0 and $(n-i)$ times at $h$, second it is positive on $]0, h[$, see *e.g.*, [10, 11, 8, 13]. The normalisation property means that $\sum_{i=0}^{n} B_i = \mathbb{1}$, where $\mathbb{1}$ stands for the constant function $\mathbb{1}(x) = 1$, for all $x$ in any working interval. Any given points $P_0, \ldots, P_n \in \mathbb{R}^d$ are called *the Bézier points relative to* $(0, h)$ of the function $F \in {\mathbb{E}_n}^d$ defined by

$$F(x) = \sum_{i=0}^{n} B_i(x)\, P_i, \quad x \in \mathbb{R}\,. \tag{1}$$

The polygon $[P_0, \ldots, P_n]$ is called the *control polygon* of $F$ on $[0, h]$.

The situation we examine subsequently is the following one:

$$\mathbb{1} \in \mathbb{E}_n \subset \mathbb{E}^\star_{n+2}, \quad \text{where } \mathbb{E}^\star_{n+2} = \ker \mathcal{L}^\star_{n+2}, \text{ with } \mathcal{L}^\star_{n+2} = p^\star_{n+2}(D). \tag{2}$$

The previous relations mean that

$$p_n(0) = 0, \quad p^\star_{n+2} = p_n q_2, \quad \text{where } q_2 \text{ is a real polynomial of degree 2.} \tag{3}$$

If $q_2$ has two real roots, say $a_1, a_2 \in \mathbb{R}$, we can insert an $(n+2)$-dimensional space $\mathbb{E}^\sharp_{n+1}$ between $\mathbb{E}_n$ and $\mathbb{E}^\star_{n+2}$, *e.g.*,

$$\mathbb{E}^\sharp_{n+1} := \ker \mathcal{L}^\sharp_{n+1}, \quad \text{where } \mathcal{L}^\sharp_{n+1} = p^\sharp_{n+1}(D), \quad \text{with } \; p^\sharp_{n+1}(x) = (x - a_1) p_n(x).$$

One can then show that the corresponding critical length for design satisfy

$$\widetilde{\ell}_n \leqslant \widetilde{\ell}^\sharp_{n+1} \leqslant \widetilde{\ell}^\star_{n+2}.$$

Moreover, on $[0, h]$, with $0 < h < \widetilde{\ell}_n$, the control polygon $[P_0, \ldots, P_n]$ on $[0, h]$ of a function $F \in {\mathbb{E}_n}^d$ is classically transformed into the control polygons on the same interval of the same function $F$ considered successively as an element of ${\mathbb{E}^\sharp_{n+1}}^d$, ${\mathbb{E}^\star_{n+2}}^d$, say respectively $[P^\sharp_0, \ldots, P^\sharp_{n+1}]$, and $[P^\star_0, \ldots, P^\star_{n+2}]$. Each of these transformations is corner-cutting as is well known [16, 15]. More precisely, there exist real numbers $\alpha_1, \ldots, \alpha_n, \beta_1, \ldots, \ldots, \beta_{n+1} \in ]0, 1[$, independent of $F$, such that

$$P^\sharp_i = (1 - \alpha_i) P_{i-1} + \alpha_i P_i \;\text{ for } i = 1, \ldots, n, \quad P^\star_i = (1 - \beta_i) P^\sharp_{i-1} + \beta_i P^\sharp_i \;\text{ for } i = 1, \ldots, n+1,$$

in addition to the equalities $P^\star_0 = P^\sharp_0 = P_0$, $P^\star_{n+2} = P^\sharp_{n+1} = P_n$. Being corner-cutting, this process is shape preserving: if the initial planar control polygon $[P_0, \ldots, P_n]$ is convex (resp. monotone in one direction), so are successively $[P^\sharp_0, \ldots, P^\sharp_{n+1}]$ and $[P^\star_0, \ldots, P^\star_{n+2}]$.

Consider again the situation (2), but now under the assumption that the roots of $q_2$ are complex numbers $a \pm ib$, with $b > 0$. Except in the trivial case where $\widetilde{\ell}_n = +\infty$, no general rule can be stated for the comparison of the critical lengths for design $\widetilde{\ell}_n$, $\widetilde{\ell}^\star_{n+2}$. We can encounter any of the three situations $\widetilde{\ell}_n = \widetilde{\ell}^\star_{n+2}$, $\widetilde{\ell}_n < \widetilde{\ell}^\star_{n+2}$, $\widetilde{\ell}_n > \widetilde{\ell}^\star_{n+2}$, as will be observed in next section. **Selecting a positive** $h < \min\left(\widetilde{\ell}_n, \widetilde{\ell}^\star_{n+2}\right)$, we investigate the associated *dimension elevation procedure* transforming the initial control polygon $[P_0, \ldots, P_n]$ of any given function $F \in {\mathbb{E}_n}^d$ into the control polygon $[P^\star_0, \ldots, P^\star_{n+2}]$ of the same function $F$ considered as an element of ${\mathbb{E}^\star_{n+2}}^d$. There are still infinitely many ways to insert an $(n+2)$-dimensional space $\mathbb{E}^\sharp_{n+1}$ between $\mathbb{E}_n$ and $\mathbb{E}^\star_{n+2}$, but none is the kernel of a linear differential operator of order $(n+2)$ with constant real coefficients. We can split the investigation into two cases [12]:

1) **Suppose that** $h < \min\left(\frac{\pi}{b}, \widetilde{\ell}_n, \widetilde{\ell}^\star_{n+2}\right)$. In that case, it is possible to select such a space $\mathbb{E}^\sharp_{n+1}$ so that $\mathbb{E}^\sharp_{n+1}$ is a W-space, not on the whole of $\mathbb{R}$, but on $[0, h]$. The inclusion (2) automatically guarantees that it is an EC-space good for design on $[0, h]$. Accordingly, we can again split the dimension elevation procedure from $\mathbb{E}_n$ to $\mathbb{E}^\star_{n+2}$ on $[0, h]$, into two elementary dimension elevation steps on $[0, h]$: first, from $\mathbb{E}_n$ to $\mathbb{E}^\sharp_{n+1}$, then from $\mathbb{E}^\sharp_{n+1}$ to $\mathbb{E}^\star_{n+2}$. As in the previous case, the procedure is thus shape preserving.

2) **Suppose that** $\frac{\pi}{b} \leqslant h < \min\left(\widetilde{\ell}_n, \widetilde{\ell}^\star_{n+2}\right)$. Then, among all possible $(n+2)$-dimensional spaces $\mathbb{E}^\sharp_{n+1}$ which can be inserted between $\mathbb{E}_n$ and $\mathbb{E}^\star_{n+2}$, none is a W-space on the interval $[0, h]$. It is therefore impossible to split the dimension elevation procedure from $\mathbb{E}_n$ to $\mathbb{E}^\star_{n+2}$ on $[0, h]$ into two elementary dimension elevation steps on $[0, h]$.

Apart from one illustration of the splitting described in case 1), our attention will be entirely focussed on case 2). The examples presented in next section are some among those which we have investigated in an attempt to try and conjecture when dimension elevation remains shape preserving. So far we are not able to state any such conjecture. We considered it useful to give access to more examples than the very few included in [4] to convince readers that, most of the time, when $h \to \min\big(\widetilde{\ell}_n, \widetilde{\ell}^\star_{n+2}\big)^-$, the dimension elevation process is no longer shape preserving, and it may even "explode" far from the initial control polygon.

# 2 Illustrations

In this section we complement some illustrations shown in [4] concerning the dimension elevation process (2). As announced in Section 1, we work under the assumption that the roots of the degree two polynomial $q_2$ involved in (3) are the complex numbers $a \pm ib$, where $b > 0$, on any given interval $[0, h]$, with of course $0 < h < \min\big(\widetilde{\ell}_n, \widetilde{\ell}^\star_{n+2}\big)$. Obviously, this requires the knowledge of the critical lengths for design $\widetilde{\ell}_n, \widetilde{\ell}^\star_{n+2}$ of the two spaces $\mathbb{E}_n, \mathbb{E}^\star_{n+2}$, respectively. In most examples, a necessary preliminary work therefore consisted in determining them, which was done through the numerical procedure built in [3].

The illustrations were initially planned to help us conjecture when the dimension elevation process remained shape preserving on the whole of $]0, \min\big(\widetilde{\ell}_n, \widetilde{\ell}^\star_{n+2}\big)[$. However the rather many subsequent examples are also intended to illustrate possible "shape effects" due to the loss of shape preservation.

## 2.1 Basic example: from polynomial to cycloidal spaces

Our first concern was to get a visual confirmation of our intuition that dimension elevation was not always shape preserving, and therefore not always corner-cutting. With this in mind, we first considered the most natural example, that is,

$$p_n(x) = x^{n+1}, \quad p^\star_{n+2}(x) = (x^2 + 1)p_n(x).$$

The initial space $\mathbb{E}_n$ is thus the degree $n$ polynomial space $\mathbb{P}_n$, while the final one $\mathbb{E}^\star_{n+2}$ is the $(n+3)$-dimension *cycloidal space* (also sometimes named *trigonometric space*) spanned by $\mathbb{P}_n$ and the two functions $\cos x, \sin x$. This is the most natural example first because it concerns the simplest possible initial space and the simplest possible polynomial $q_2$, but also because we know the critical lengths of all cycloidal spaces. These critical lengths have been investigated in several articles [5, 6] and they were definitively determined in relation with the first positive zeroes of Bessel functions in [7], see also [1, 3]. In particular, we thus have, in addition to $\widetilde{\ell}_2 = \pi$,

$$\widetilde{\ell}^\star_3 = \widetilde{\ell}^\star_4 = 2\pi, \quad \widetilde{\ell}^\star_5 = \widetilde{\ell}^\star_6 \approx 8.9868, \quad \widetilde{\ell}^\star_7 = \widetilde{\ell}^\star_8 \approx 11.5269, \quad \ldots \tag{4}$$

According to case 1) in Section 1, we know that, for any $h < \pi$, we can split the dimension elevation from $\mathbb{E}_n$ to $\mathbb{E}^\star_{n+2}$ on $[0, h]$ into two elementary dimension elevation steps corresponding to the insertion of an $(n+2)$-dimensional space $\mathbb{E}^\sharp_{n+1}$ between $\mathbb{E}_n$ and $\mathbb{E}^\star_{n+2}$, chosen so that it will be a W-space on $[0, h]$. In order to ensure the symmetry of the intermediate space $\mathbb{E}^\sharp_{n+1}$, we define it as

$$\mathbb{E}^\sharp_{n+1} := \operatorname{span}(\mathbb{E}_n, U),$$

where the function $U$ is defined on $[0, h]$ as follows:

$$U(x) := \sin x + \sin(h - x) \text{ if } n \text{ is odd}, \quad U(x) := \cos x - \cos(h - x) \text{ if } n \text{ is even}. \tag{5}$$

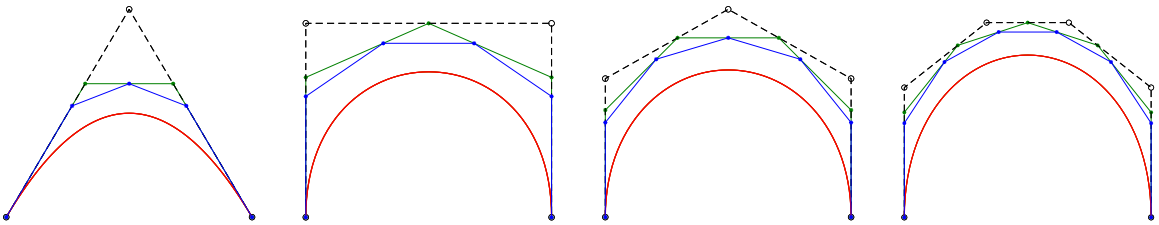

Figure 1: Two-step corner cutting dimension elevation algorithm on $[0, h]$, with $h < \pi$, obtained by inserting $\mathbb{E}^\sharp_{n+1} := \mathrm{span}(\mathbb{P}_n, U)$ between $\mathbb{P}_n$ and $\mathbb{E}^*_{n+2} = \mathrm{span}(\mathbb{P}_n, \cos, \sin)$, with $U$ defined in (5). Here $h = 2$.

This is illustrated in Fig. 1, with $h = 2$, and successively $n = 2; 3; 4; 5$.

In Figure 2, we illustrate Case 2) successively for $n = 2; 3; 4; 5; 6$. For each value of $n$, dimension elevation from the polynomial space $\mathbb{E}_n$ to the cycloidal space $\mathbb{E}^\star_{n+2}$ is shown on $[0, h]$, with increasing values of $h$ from $\pi^+$ to $\ell^{\star -}_{n+1} = \widetilde{\ell}^{\star -}_{n+2}$. As is logical we observe that for $h$ close to $\pi^+$, we have visual shape preservation. Oppositely, when approaching $\widetilde{\ell}^\star_{n+2}$, we clearly lose shape preservation, with similar behaviour depending on the parity of $n$. Close to $\widetilde{\ell}^\star_{n+2}$, the central (two) point(s) are even located very far outside the convex hull of the initial control polygon.

## 2.2 Example 2: $\widetilde{\ell}_n < \widetilde{\ell}^\star_{n+2}$ versus $\widetilde{\ell}_n > \widetilde{\ell}^\star_{n+2}$?

As mentioned in Section 1, any sequence of elementary dimension elevation steps automatically increases the critical lengths for design. Now, in the previous series of examples we were always in the situation $\widetilde{\ell}_n = +\infty > \widetilde{\ell}^\star_{n+2}$. It was therefore necessary to check whether the loss of shape preservation was attached to the decrease of the critical lengths for design as the dimension increases. With this in mind, we fixed $n = 4$ and considered the dimension elevation $\mathbb{E}_4 \subset \mathbb{E}^\star_6$, corresponding to the characteristic polynomials

$$p_4(x) := x(x^2 + 1)^2, \quad p_6(x) := p_4(x)(x^2 + b^2) \ \text{ for some } b > 0.$$

The space $\mathbb{E}_4$ is spanned by the functions $1, \cos x, \sin x, x\cos x, x \sin x$, and $\mathbb{E}^\star_6$ by $\mathbb{E}_4$ and the two functions $\cos(bx), \sin(bx)$ if $b \neq 1$ (resp., $x^2 \cos x, x^2 \sin x$ for $b = 1$). Through the numerical procedure in [3] we obtain:

$$\widetilde{\ell}_4 \approx 4.4934.$$

Since we want to provide illustrations only when

$$\pi/b < h < \min\big(\widetilde{\ell}_4, \widetilde{\ell}^\star_6\big), \tag{6}$$

we will investigate dimension elevation from $\mathbb{E}_4$ to $\mathbb{E}^\star_6$ only for values of $b > \pi/\widetilde{\ell}_4$, that is, in practice $b \geqslant 0.7$. We first selected a sequence of values of $b \geqslant 0.7$, and for each of them, we applied the numerical procedure to calculate the critical length for design $\widetilde{\ell}^\star_6$, and then investigated the dimension elevation procedure. The selected values were successively $b = 0.7; 0.9; 1.1; 1.5; 2; 3; 6$. We could observe two different behaviours. For $b = 0.7; 0.9; 1.1; 1.5$, the central final control point $P^\star_3$ is immediately attracted towards the central initial control point $P_2$ as $h$ increases, and the process seems visually shape preserving until $\min\big(\widetilde{\ell}_4, \widetilde{\ell}^\star_6\big)^-$. On the contrary, for $b = 2; 3; 6$, $P^\star_3$ is repulsed from $P_2$ and we lose shape preservation when approaching the limit for $h$. Moreover in the latter case, the "non-shape preservation" effects are quite similar to those shown in Figure 2, line 3. This

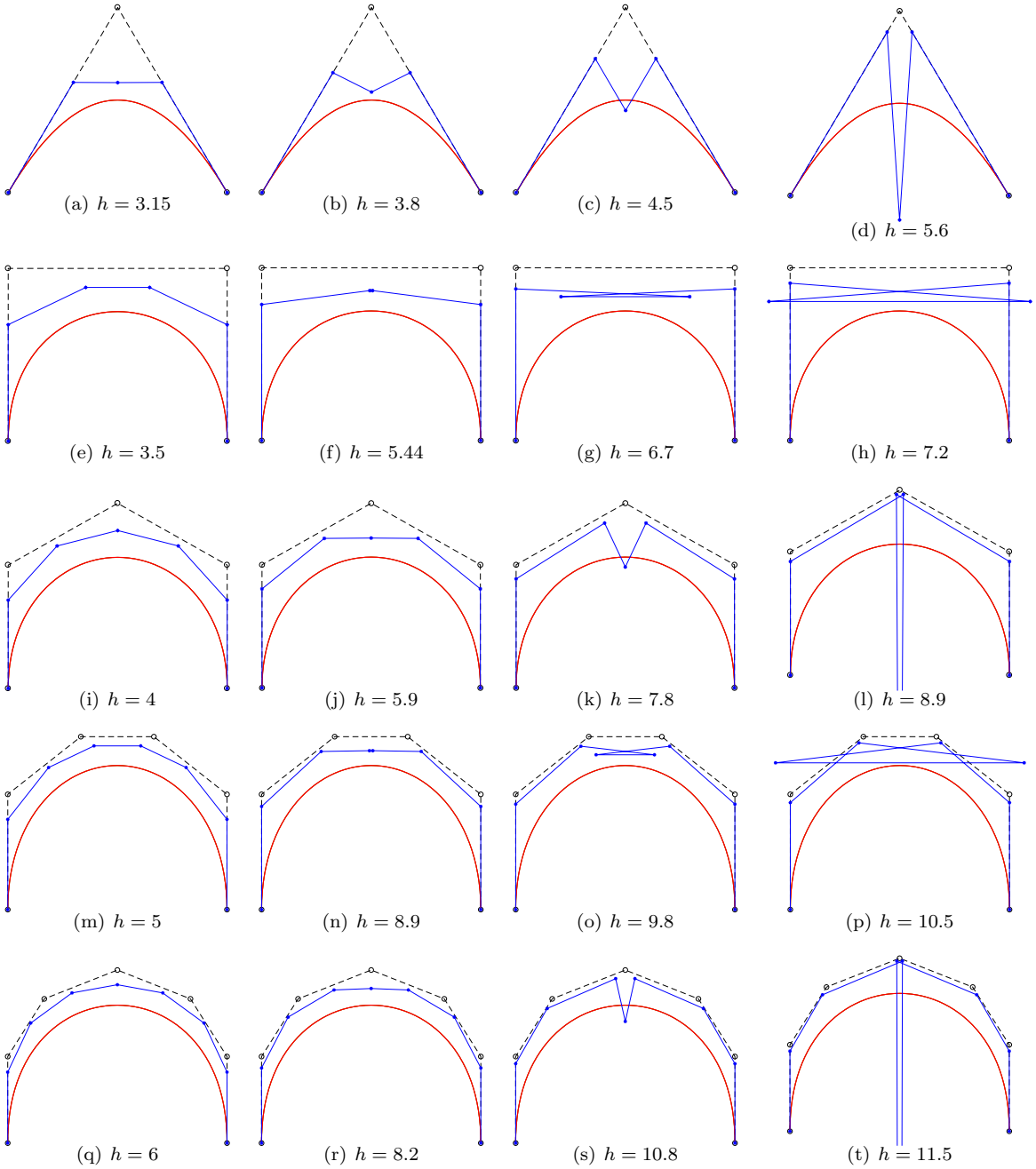


Figure 2: For increasing values of $n$, dimension elevation $\mathbb{E}_n \subset \mathbb{E}_{n+2}$, where $\mathbb{E}_n$ is the degree $n$ polynomial space $\mathbb{P}_n$ and $\mathbb{E}_{n+2}$ is the cycloidal space spanned by $\mathbb{P}_n$ and the two functions $\cos, \sin$, on $[0, h]$, with $\pi < h < \widetilde{\ell}^{\star}_{n+2}$. For the values of $\widetilde{\ell}^{\star}_{n+2}$, see (4).

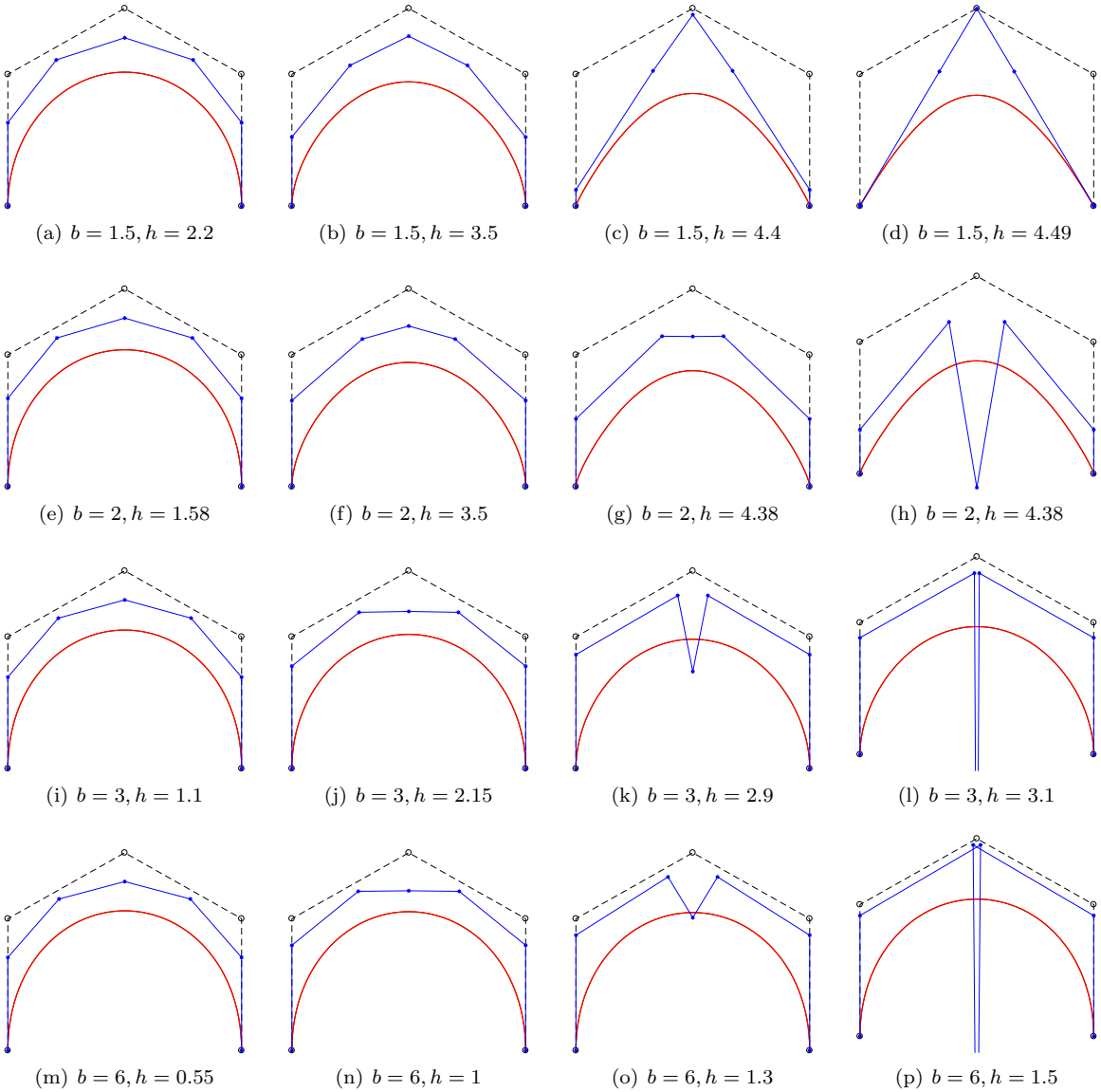

(a) $b = 1.5, h = 2.2$ (b) $b = 1.5, h = 3.5$ (c) $b = 1.5, h = 4.4$ (d) $b = 1.5, h = 4.49$

(e) $b = 2, h = 1.58$ (f) $b = 2, h = 3.5$ (g) $b = 2, h = 4.38$ (h) $b = 2, h = 4.38$

(i) $b = 3, h = 1.1$ (j) $b = 3, h = 2.15$ (k) $b = 3, h = 2.9$ (l) $b = 3, h = 3.1$

(m) $b = 6, h = 0.55$ (n) $b = 6, h = 1$ (o) $b = 6, h = 1.3$ (p) $b = 6, h = 1.5$

Figure 3: Dimension elevation $\mathbb{E}_4 \subset \mathbb{E}_6^\star$, with $p_4 = x(x^2+1)^2$, $p_6(x) = p_4(x)(x^2+b^2)$, $b>1$. We have $\widetilde{\ell}_4 \approx 4.4934$ and, from top to bottom, $(b, \widetilde{\ell}_6^\star, \pi/b) = (1.5, 5.0331, 2.0944)$; $(2, 4.3965, 1.5708)$; $(3, 3.1415, 1.0472)$; $(6, 1.5247, 0.5236)$.

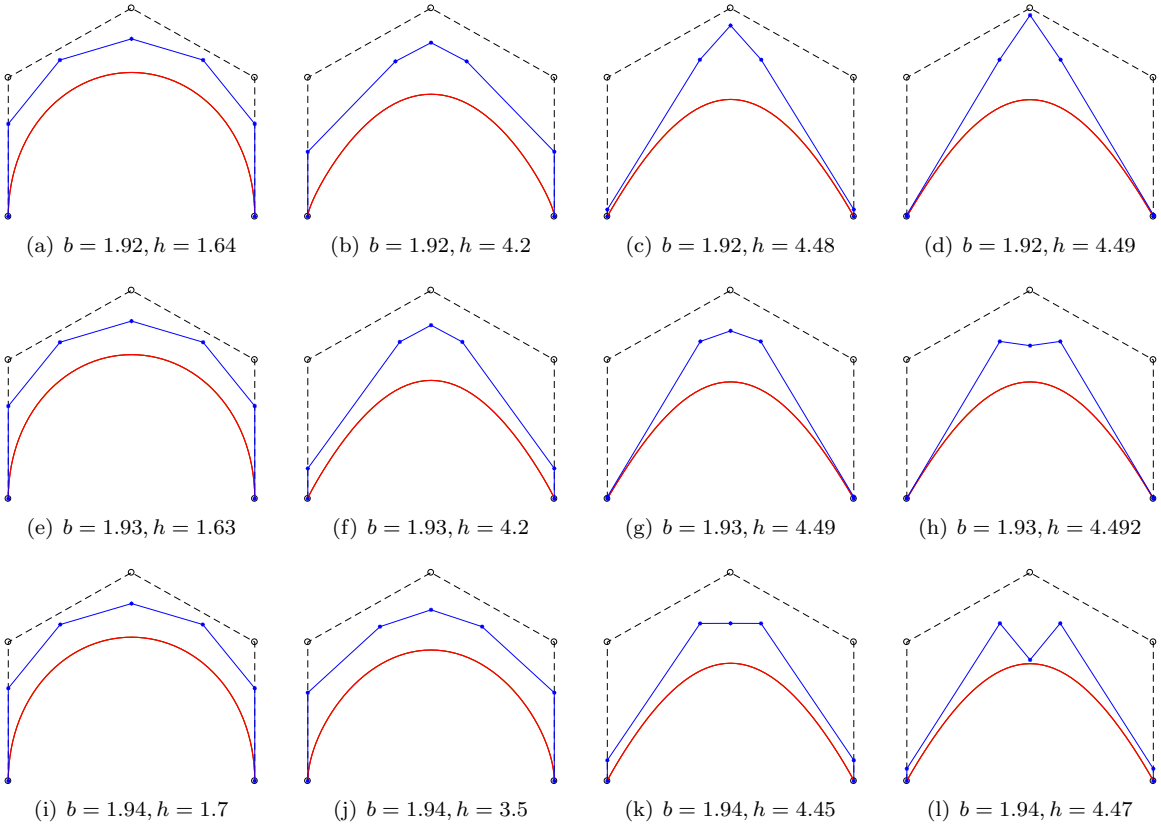

(a) $b = 1.92, h = 1.64$ (b) $b = 1.92, h = 4.2$ (c) $b = 1.92, h = 4.48$ (d) $b = 1.92, h = 4.49$

(e) $b = 1.93, h = 1.63$ (f) $b = 1.93, h = 4.2$ (g) $b = 1.93, h = 4.49$ (h) $b = 1.93, h = 4.492$

(i) $b = 1.94, h = 1.7$ (j) $b = 1.94, h = 3.5$ (k) $b = 1.94, h = 4.45$ (l) $b = 1.94, h = 4.47$

Figure 4: Same as Figure 3, but with, $(b, \widetilde{\ell}_6^\star, \pi/b) = (1.92, 4.5066, 1.6362)$; $(1.93, 4.4928, 1.6278)$; $(1.94, 4.4790, 1.6194)$;

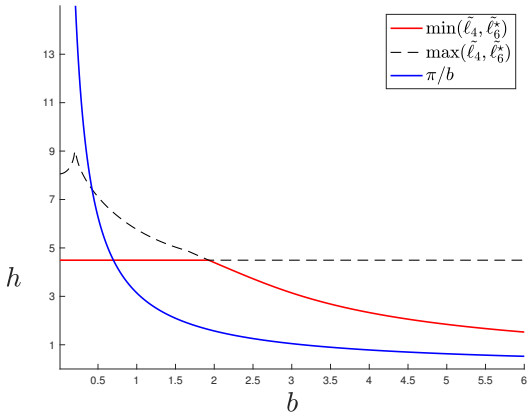


Figure 5: The region $\pi/b < h < \min(\widetilde{\ell}_4, \widetilde{\ell}_6^\star)$ within which we experiment in Figs. 3 and 4.

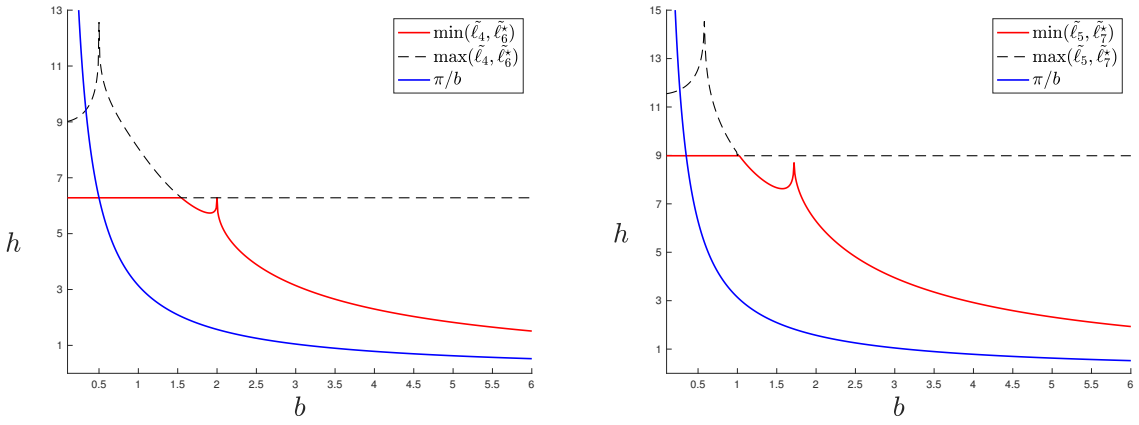


Figure 6: The region $\pi/b < h < \min(\widetilde{\ell}_n, \widetilde{\ell}_{n+2}^\star)$ corresponding to (7). Left: $n = 4$. Right: $n = 5$.

can be observed in Figure 3, in which we do not show the values $b = 0.7; 0.9; 1.1$ which do not provide any novelty by comparison to the limit final polygon obtained with $b = 1.5$.

In the caption of Figure 3, for each value of $b$ we indicate the value of $\pi/b$ and $\widetilde{\ell}_6^\star$. It can be observed that, for $b = 1.5$, $\widetilde{\ell}_6^\star > \widetilde{\ell}_4$ (this is also true for the smaller values of $b$) whereas, for $b \geqslant 2$, we have $\widetilde{\ell}_6^\star < \widetilde{\ell}_4$. This is why in a second step, we refined the experimentation in the interval $[1.5, 2]$, and more precisely around the value $b \approx 1.93^-$, numerically determined through the numerical procedure in [3], for which the equality $\widetilde{\ell}_6^\star = \widetilde{\ell}_4$ is satisfied. We can see in Figure 4 that the change between the attraction / repulsion phenomenon is located in between 1.92 and 1.93, and even closer to 1.93: indeed, in order to observe the loss of shape preservation we had to work with $h$ very close to $\widetilde{\ell}_6^\star$.

This experimentation naturally led us to state the following conjecture:

Conjecture: *the dimension elevation procedure remains shape preserving for all admissible values of $h$ if and only $\widetilde{\ell}_6^\star > \widetilde{\ell}_4$.*

It can be useful to the reader to see the graph of the critical length for design $\widetilde{\ell}_6^\star$ as a function of the positive parameter $b$. It is shown in Figure 5, along with the region (6) of the plane $(b, h)$ that we investigated.

## 2.3 Example 3: contradict the conjecture

To try and confirm / contradict the previous conjecture we investigated in particular the case:

$$p_n(x) := x^{n-1}(x^2 + 1), \quad p_{n+2}^\star(x) := p_n(x)(x^2 + b^2), \text{ with } b > 0. \tag{7}$$

In other words, $\mathbb{E}_n$ is the $(n+1)$-dimensional cycloidal space, and $\mathbb{E}_{n+2}^\star$ is spanned by $\mathbb{E}_n$ and the two functions $\cos(bx), \sin(bx)$ if $b \neq 1$, and $x\cos x, x\sin x$ if $b = 1$.

The few examples we considered with $n = 3$ seemed to visually confirm the conjecture. We then tried succesively $n = 4$ and $n = 5$. In Figure 6 we present the graph of the critical length $\widetilde{\ell}_{n+2}^\star$ as a function of the positive parameter $b$ and the region $\pi/b < h < \min\big(\widetilde{\ell}_n, \widetilde{\ell}_{n+2}^\star\big)$ for $n = 4; 5$. The case $n = 4$ is illustrated in Figures 7 and 8. Note that the equality $2\pi = \widetilde{\ell}_4 = \widetilde{\ell}_6^\star$ is obtained for $b \approx 1.545$. For all values of $b$ considered in Figure 7, we have $\widetilde{\ell}_4 < \widetilde{\ell}_6^\star$. Still, visually speaking, we already lose shape preservation as $h$ increases in the third line of Figure 7, that is, for $b = 1.2$, thus clearly

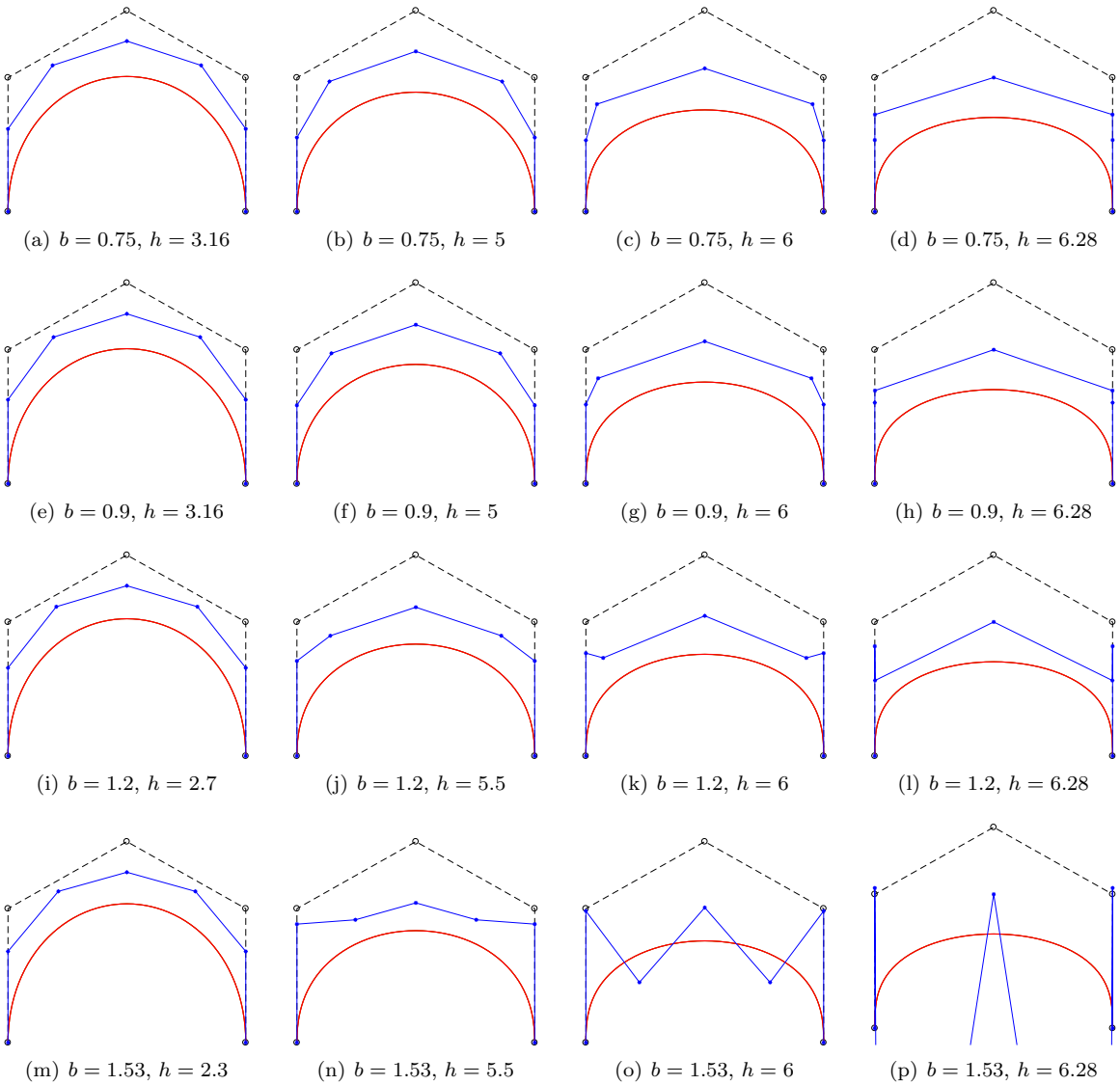

(a) $b = 0.75$, $h = 3.16$ (b) $b = 0.75$, $h = 5$ (c) $b = 0.75$, $h = 6$ (d) $b = 0.75$, $h = 6.28$

(e) $b = 0.9$, $h = 3.16$ (f) $b = 0.9$, $h = 5$ (g) $b = 0.9$, $h = 6$ (h) $b = 0.9$, $h = 6.28$

(i) $b = 1.2$, $h = 2.7$ (j) $b = 1.2$, $h = 5.5$ (k) $b = 1.2$, $h = 6$ (l) $b = 1.2$, $h = 6.28$

(m) $b = 1.53$, $h = 2.3$ (n) $b = 1.53$, $h = 5.5$ (o) $b = 1.53$, $h = 6$ (p) $b = 1.53$, $h = 6.28$

Figure 7: Dimension elevation on $[0, h]$ from $\mathbb{E}_4$ to $\mathbb{E}_6^\star$, with $p_4(x) = x^3(x^2 + 1)$ ($\widetilde{\ell}_4 = 2\pi$), and $p_6(x) = p_4(x)(x^2 + b^2)$. From top to bottom, $(b, \widetilde{\ell}_6^\star, \pi/b) = (0.75, 9.1503)$; $(0.9, 8.4715)$; $(1.2, 7.3016, 2.6180)$; $(1.53, 6.3229, 2.0533)$.

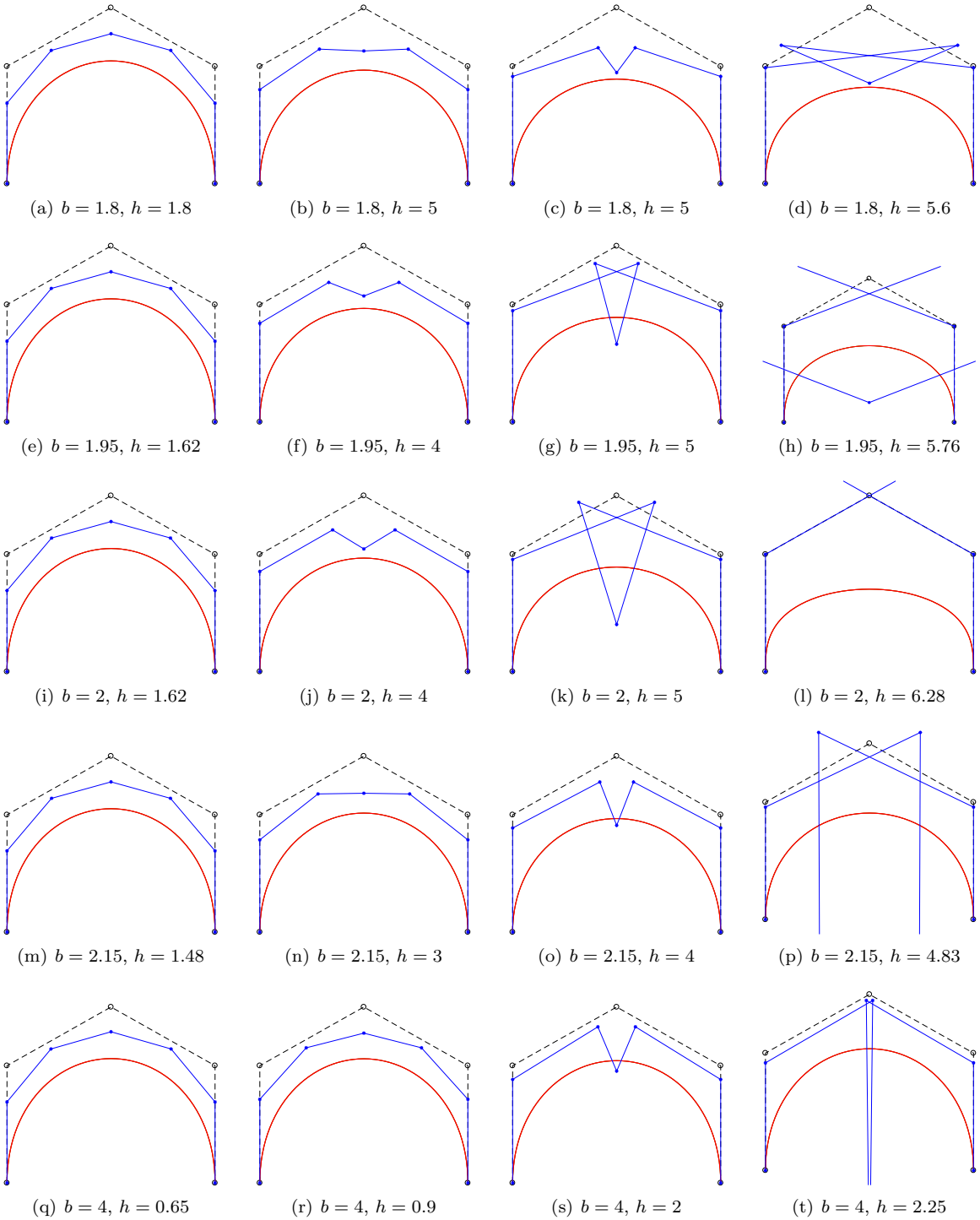

(a) $b = 1.8$, $h = 1.8$ (b) $b = 1.8$, $h = 5$ (c) $b = 1.8$, $h = 5$ (d) $b = 1.8$, $h = 5.6$

(e) $b = 1.95$, $h = 1.62$ (f) $b = 1.95$, $h = 4$ (g) $b = 1.95$, $h = 5$ (h) $b = 1.95$, $h = 5.76$

(i) $b = 2$, $h = 1.62$ (j) $b = 2$, $h = 4$ (k) $b = 2$, $h = 5$ (l) $b = 2$, $h = 6.28$

(m) $b = 2.15$, $h = 1.48$ (n) $b = 2.15$, $h = 3$ (o) $b = 2.15$, $h = 4$ (p) $b = 2.15$, $h = 4.83$

(q) $b = 4$, $h = 0.65$ (r) $b = 4$, $h = 0.9$ (s) $b = 4$, $h = 2$ (t) $b = 4$, $h = 2.25$

Figure 8: Same as Figure 7, with, from top to bottom, $(b, \widetilde{\ell}_6^\star, \pi/b) = (1.8, 5.8156, 1.7453)$; $(1.95, 5.7633, 1.6111)$; $(2, 6.2827, 1.5708)$; $(2.15, 4.8334, 1.4612)$; $(4, 2.3005, 0.7853)$.

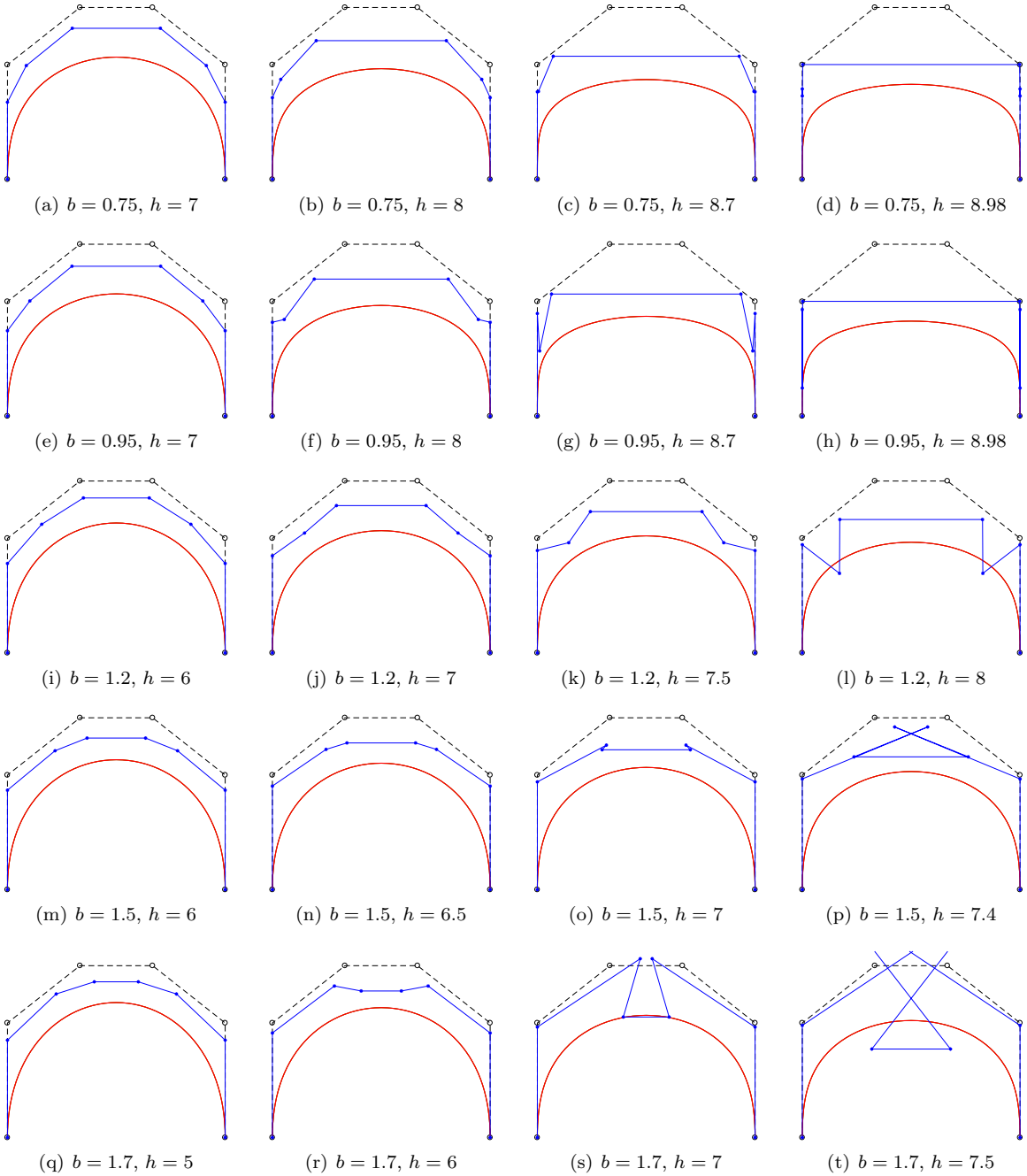

(a) $b = 0.75$, $h = 7$ (b) $b = 0.75$, $h = 8$ (c) $b = 0.75$, $h = 8.7$ (d) $b = 0.75$, $h = 8.98$

(e) $b = 0.95$, $h = 7$ (f) $b = 0.95$, $h = 8$ (g) $b = 0.95$, $h = 8.7$ (h) $b = 0.95$, $h = 8.98$

(i) $b = 1.2$, $h = 6$ (j) $b = 1.2$, $h = 7$ (k) $b = 1.2$, $h = 7.5$ (l) $b = 1.2$, $h = 8$

(m) $b = 1.5$, $h = 6$ (n) $b = 1.5$, $h = 6.5$ (o) $b = 1.5$, $h = 7$ (p) $b = 1.5$, $h = 7.4$

(q) $b = 1.7$, $h = 5$ (r) $b = 1.7$, $h = 6$ (s) $b = 1.7$, $h = 7$ (t) $b = 1.7$, $h = 7.5$

Figure 9: Dimension elevation on $[0, h]$ from $\mathbb{E}_5$ to $\mathbb{E}_7^\star$, with $p_5(x) = x^3(x^2 + 1)$ ($\widetilde{\ell}_5 = 8.9868$), and $p_7(x) = p_5(x)(x^2 + b^2)$. From top to bottom, $(b, \widetilde{\ell}_7^\star, \pi/b) = (0.75, 10.6131, 4.1888)$; $(0.95, 9.3339, 3.3069)$; $(1.2, 8.3302, 2.6180)$; $(1.5, 7.6659, 2.0944)$; $(1.7, 8.0270, 1.8480)$.

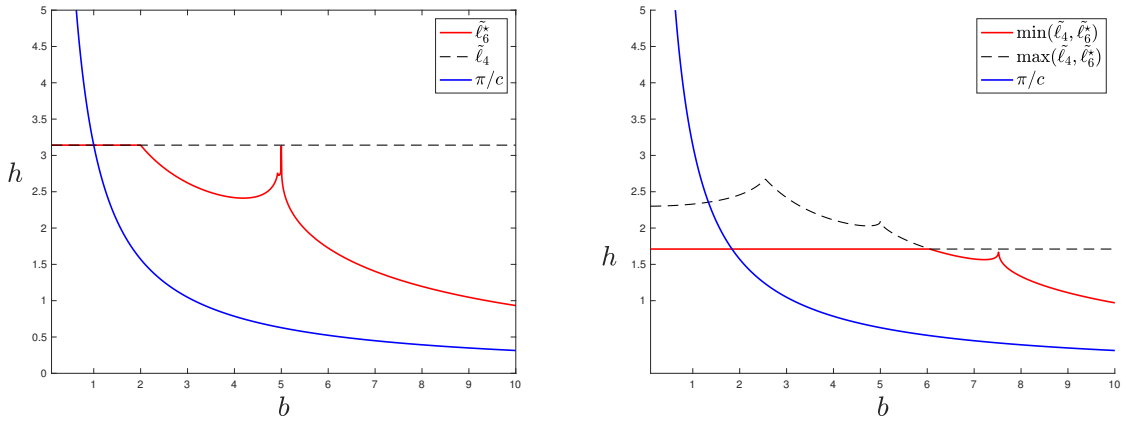


Figure 10: The region $\pi/b < h < \min(\widetilde{\ell}_4, \widetilde{\ell}_6^\star)$, with $p_6(x) := p_4(x)(x^2+b^2)$. Left: $p_4(x) = x(x^2+1)(x^2+9)$, for which $\widetilde{\ell}_4 = \pi$. Right: $p_4(x) = x(x^2+1)(x^2+16)$, for which $\widetilde{\ell}_4 \approx 1.7108$.

contradicting the conjecture. In Figure 8, we always have $\widetilde{\ell}_4 > \widetilde{\ell}_6^\star$. In these two figures, we illustrate what happens for many values of $b$, for the loss of shape preservation results in many different ways depending on $b$. For higher values (see $b = 4$) we recover shapes more similar to Figure 2, line 3.

In Figure 9 we similarly present several examples for $n = 5$, confirming again that the conjecture was false. Indeed, for $b = 0.95$ we can see that we lose shape preservation in the limit, though $\widetilde{\ell}_7^\star > \widetilde{\ell}_5$.

## 2.4 A few additional examples

One of the first examples we investigated was the case $\mathbb{E}_3 \subset \mathbb{E}_5^\star$, with $\mathbb{E}_3$ spanned by the functions $1, x, \cos x, \sin x$, and $\mathbb{E}_5^\star$ obtained by "adding" the two functions, $x\cos x$, $x\sin x$, that is $p_3(x) = x^2(x^2+1)$ and $p_5(x) = x^2(x^2+1)^2$. In that case we have $\widetilde{\ell}_3 = \widetilde{\ell}_5^\star = 2\pi$ and the dimension elevation procedure visually seems shape preserving. However, the initial control polygon $[P_0, \dots, P_3]$ being given, it is well known that the corresponding curve in $\mathbb{E}_3$ "tends to" the segment $[P_0, P_3]$ as $h$ approaches $2\pi^-$, and the same holds true with the final control polygon, which does not facilitate visual appreciation of what happens. On the other hand, we have already encountered examples for which the initial and final critical lengths for design were equal with no shape preservation close to them. It was therefore worthwhile considering more examples with same initial and final critical lengths for design.

Recall that the three spaces respectively spanned by the functions $1, \cos x, \sin x, \cos(2x), \sin(2x)$, the functions $1, \cos x, \sin x, \cos(3x), \sin(3x)$, and the functions $1, \cos x, \sin x, \cos(2x), \sin(2x), \cos(3x)$, $\sin(3x)$, have the same critical lengths for design equal to $\pi$, see for instance [3]. This is why we considered the whole class of dimension elevation procedures attaches to

$$\mathbb{E}_4 \subset \mathbb{E}_6^\star, \quad \text{with} \quad p_4(x) := x(x^2+1)(x^2+9) \quad \text{and} \quad p_6^\star = p_4(x)(x^2+b^2), \tag{8}$$

for some positive $b$. One specific advantage of this class is that, whatever the positive $b$, we are always in the situation

$$\pi = \widetilde{\ell}_4 \geqslant \widetilde{\ell}_6^\star. \tag{9}$$

Indeed, the non-zero function $U \in D\mathbb{E}_6^\star$ defined by $U(x) = 3\sin x - \sin(3x)$ vanishes 6 times on $[0, \pi]$ since

$$U(0) = U'(0) = U''(0) = U(\pi) = U'(\pi) = U''(\pi) = 0.$$

That (9) is true for any $b > 0$ is confirmed by the graph of the critical length for design $\widetilde{\ell}_6$ in function of $b$ shown in Figure 10, left. Some examples of dimension elevation are shown in Figure 11. For $b = 1.5$ and $h = \pi^-$, the curve cannot be distinguished from the segment $[P_0, P_4]$ nor the points $P_1^\star, P_2^\star$ from $P_0$, and symmetrically for $P_4^\star, P_5^\star$. The procedure seems to remain shape preserving until the limit, which we could confirm by strongly zooming at $P_0$. All along the horizontal red segment in Figure 10, left, that it, for $b \in [1, 2]$, (for $b < 1$ we are under the blue hyperbola) the limit control polygon is similar to the one obtained with $b = 1.5$ and a convenient zoom at $P_0$ convinced us that we always have visual shape preservation. We could verify that, as soon as $b > 1$, this property is no longer satisfied.

The graph of $\widetilde{\ell}_6^\star$ presents two cusps close to each other, the second one being at $b = 5$. Observe the difference between the "shape effects" of the non shape preservation at $b = 3.5; 4$ on the one hand, and at $b = 6; 12$ on the other. These values correspond to two different smooth parts of the curve, see Section 3.

In Figure 10, right, we can see the graph of $\widetilde{\ell}_6^\star$ in function of $b$ when replacing $p_4$ in (8) by $p_4(x) = x(x^2+1)(x^2+16)$. A few associated dimension elevation illustrations are shown in Figure 12. Here too we can observe different limit behaviours before ($b = 7.5$) and after the cusp ($b = 8; 10$).

# 3 A brief analysis

Subsequently, we provide a simple geometrical understanding of the critical length for design, in relation with blossoms. It relies on the geometrical approach of EC-spaces, which naturally brings forward EC-spaces good for design.

## 3.1 Critical length for design: a geometrical description

Consider an $(n+1)$-dimensional space $\mathbb{E}_n \subset C^n(I)$, where $I$ is a given non-trivial real interval, and we assume that $\mathbb{E}_n$ contains the constants. Select a mother-function $\Phi := (\Phi_1, \dots, \dots, \Phi_n)$, in the sense that $(\mathbb{1}, \Phi_1, \dots, \dots, \Phi_n)$ is a basis of $\mathbb{E}_n$. Then, the osculating flat of any order $i \leqslant n$ at a point $x \in I$ is the affine flat going through $\Phi(x)$ and the direction of which is the linear space spanned by $\Phi'(x), \dots, \Phi^{(i)}(x)$. We denote it by $\mathrm{Osc}_i\, \Phi(x)$. The terminology $\mathbb{E}_n$ is an *EC-space good for design* was adopted relatively recently. It means that $\mathbb{E}_n$ contains the constants and possesses *blossoms*, defined in a geometrical way in terms of osculating flats. This situation, proved to be equivalent to the fact that $D\mathbb{E}_n$ is an EC-space on $I$, was deeply investigated after the initial paper by Pottmann [16], see for instance [11].

We recall below a very strong result in the geometrical approach of EC-spaces: the proof of the existence of blossoms can be reduced to the much easier proof of existence of Bézier points, according to the result recalled in Theorem 3.1 below [9].

**Theorem 3.1.** *Concerning the space $\mathbb{E}_n$ defined above, the following two properties are equivalent:*

*(1) $\mathbb{E}_n$ is an EC-space good for design on $I$;*

*(2) $\mathbb{E}_n$ is a W-space on $I$ and, for any $a, b \in I$, $a < b$, and any integer $i$, $1 \leqslant i \leqslant n-1$, the osculating flats $\mathrm{Osc}_i\, \Phi(a)$ and $\mathrm{Osc}_{n-i}\, \Phi(b)$ have a unique common point.*

When (i) is satisfied, for any $a, b \in I$, $a < b$, the points

$$\{\Pi_i(a, b)\} := \mathrm{Osc}_i\, \Phi(a) \bigcap \mathrm{Osc}_{n-i}\, \Phi(b)\ , \quad 0 \leqslant i \leqslant n, \tag{7}$$

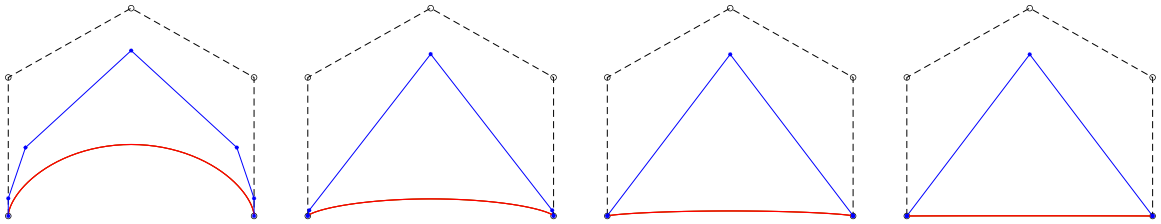

(a) $b = 1.5$, $h = 2.5$ (b) $b = 1.5$, $h = 3$ (c) $b = 1.5$, $h = 3.1$ (d) $b = 1.5$, $h = 3.14$

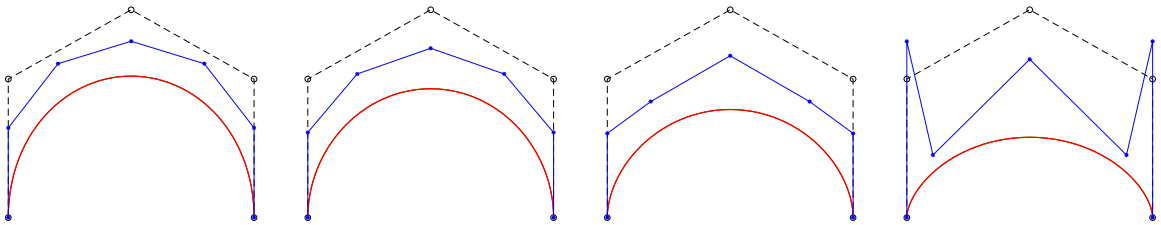

(e) $b = 3.5$, $h = 0.9$ (f) $b = 3.5$, $h = 1.5$ (g) $b = 3.5$, $h = 2$ (h) $b = 3.5$, $h = 2.4$

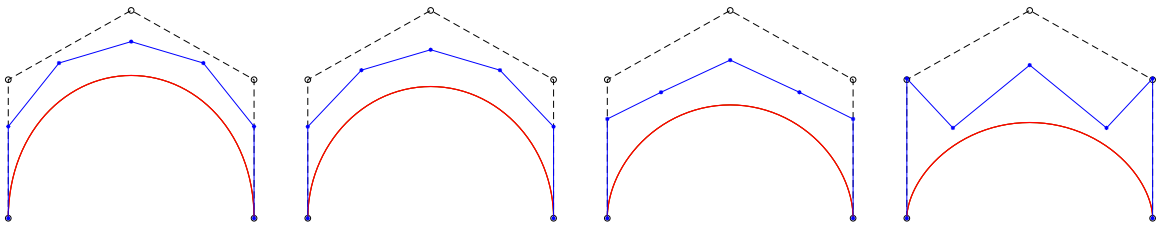

(i) $b = 4$, $h = 0.8$ (j) $b = 4$, $h = 1.4$ (k) $b = 4$, $h = 1.9$ (l) $b = 4$, $h = 2.2$

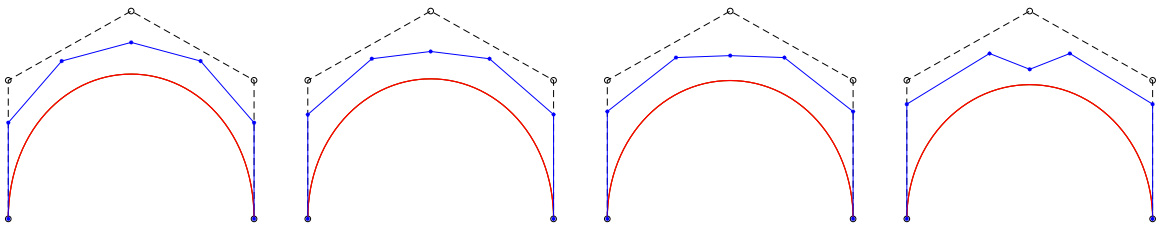

(m) $b = 6$, $h = 0.6$ (n) $b = 6$, $h = 1$ (o) $b = 6$, $h = 1.1$ (p) $b = 6$, $h = 1.3$

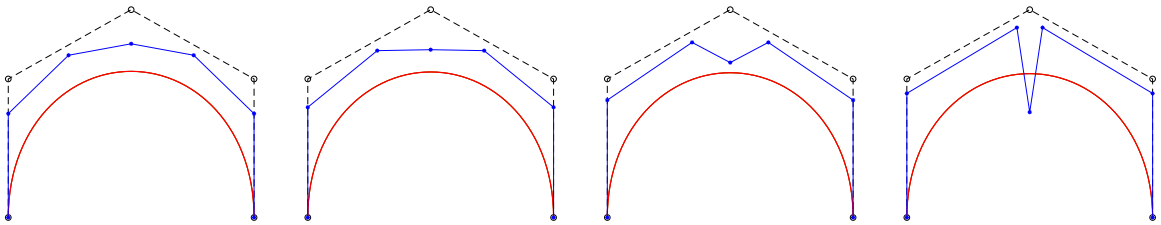

(q) $b = 12$, $h = 0.4$ (r) $b = 12$, $h = 0.5$ (s) $b = 12$, $h = 0.6$ (t) $b = 12$, $h = 0.7$

Figure 11: Dimension elevation from $\mathbb{E}_4$ to $\mathbb{E}_6^\star$ on $[0, h]$, with $p_4(x) = x(x^2 + 1)(x^2 + 9)$ ($\widetilde{\ell}_4 = \pi$) and $p_6(x) := p_4(x)(x^2 + b^2)$, see Figure 10. From top to bottom, $(b, \widetilde{\ell}_6^\star, \pi/b) = (1.5, \pi, 1)$; $(3.5, 2.4887, 0.8975)$; $(4, 2.4188, 0.7853)$; $(6, 1.7245, 0.5235)$; $(12, 0.7678, 0.2617)$.

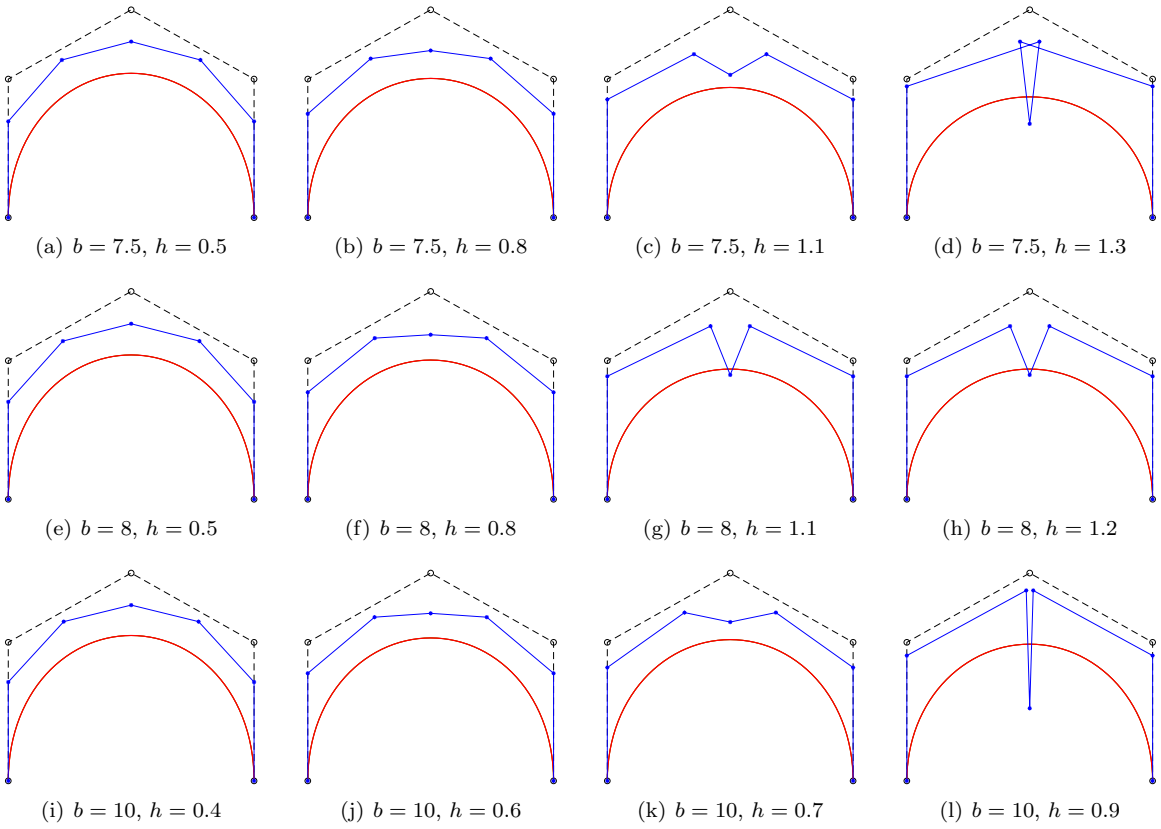

(a) $b = 7.5$, $h = 0.5$ (b) $b = 7.5$, $h = 0.8$ (c) $b = 7.5$, $h = 1.1$ (d) $b = 7.5$, $h = 1.3$

(e) $b = 8$, $h = 0.5$ (f) $b = 8$, $h = 0.8$ (g) $b = 8$, $h = 1.1$ (h) $b = 8$, $h = 1.2$

(i) $b = 10$, $h = 0.4$ (j) $b = 10$, $h = 0.6$ (k) $b = 10$, $h = 0.7$ (l) $b = 10$, $h = 0.9$

Figure 12: Dimension elevation from $\mathbb{E}_4$ to $\mathbb{E}_6^\star$ on $[0, h]$, with $p_4(x) = x(x^2+1)(x^2+16)$ ($\widetilde{\ell}_4 \approx 1.7108$) and $p_6(x) := p_4(x)(x^2+b^2)$, see Figure 10. From top to bottom $(b, \widetilde{\ell}_6^\star, \pi/b) = (7.5, 1.6239, 0.4188)$; $(8, 1.3338, 0.3926)$; $(10, 0.9704, 0.3141)$.

are the Bézier points of $\Phi$ relative to $(a,b)$, with therefore $\Pi_0(a,b)=\Phi(a)$, $\Pi_n(a,b)=\Phi(b)$, leading to the expansion (1) of the function $\Phi$ in the Bernstein basis relative to $(a,b)$. As is classical, the Bézier points relative to $(a,b)$ of any $F\in {\mathbb{E}_n}^d$ are then obtained from those of $\Phi$ via affine maps. If (ii) is not satisfied, given $a,b\in I$, $a<b$, it may still be the case that the osculating flats $\mathrm{Osc}_i\,\Phi(a)$ and $\mathrm{Osc}_{n-i}\,\Phi(b)$ have a unique common point for some integer $i$, $1\leqslant i\leqslant n-1$. The corresponding point $\Pi_i(a,b)$ will still be called the $i$th Bézier points of $\Phi$ relative to $(a,b)$. The point $\Pi_i(a,b)$ is well defined if and only if the $n$ vectors $\Phi'(a),\dots,\Phi^{(i)}(a),\Phi'(b),\dots,\Phi^{(n-i)}(b)$ are linearly independent that is, if and only if

$$\Delta_i(a,b):=\det\Big(\Phi'(a),\dots,\Phi^{(i)}(a),\Phi'(b),\dots,\Phi^{(n-i)}(b)\Big)\neq 0.$$

Let us now apply Theorem 3.1 to kernels of linear differential operators with constant real coefficients. On account of the invariance under translation, we can state:

**Theorem 3.2.** *Let $p_n$ be a polynomial of exact degree $n$, with leading coefficient one, with at least one non-real root, and with $p_n(0)=0$. Then, the critical length for design $\widetilde{\ell}_n$ of the space $\mathbb{E}_n=\ker p_n(D)$ is the minimum positive $h$ for which there exists an integer $i$, $1\leqslant i\leqslant n-1$, such that the $i$th Bézier point of a $\Phi$ relative to $(0,h)$ is not defined.*

In other words, $\widetilde{\ell}_n$, is characterised by the following two properties:

1) for $0<h<\widetilde{\ell}_n$, and for $1\leqslant i\leqslant n-1$, the Bézier point $\Pi_i(0,h)$ is well-defined; (that is, $\Delta_i(0,h)\neq 0$);

2) there exists an integer $i$, $1\leqslant i\leqslant n-1$, such that the Bézier point $\Pi_i(0,\widetilde{\ell}_n)$ does not exist (that is, such that $\Delta_i(0,\widetilde{\ell}_n)=0$).

The forcefulness of this geometrical description is that the results do not depend on the selected mother-function $\Phi$, which can therefore be chosen in an appropriate way depending on the expected result. For instance, suppose that $p_n$ is odd or even, which corresponds to the space $\mathbb{E}_n$ being symmetric, that is, closed under reflection. Then, subject to existence, for $i=1,\dots,n-1$, the $i$th Bézier point of $\Phi$ relative to $(0,h)$ is the $(n-i)$th Bézier point of $\Psi$ relative to $(0,h)$, where $\Psi(x):=\Phi(h-x)$. Accordingly, instead of considering all integers $1\leqslant i\leqslant n$ in the above properties 1) and 2), we can limit ourselves to $\frac{n}{2}\leqslant i\leqslant n-1$. This can be stated as follows.

**Corollary 3.3.** *In the same situation as in Theorem 3.2, assume that $p_n$ is either odd or even. Then, the critical length for design $\widetilde{\ell}_n$ of the space $\mathbb{E}_n=\ker p_n(D)$ is the minimum positive $h$ for which there exists an integer $i$, $\frac{n}{2}\leqslant i\leqslant n-1$, such that the $i$th Bézier point of a $\Phi$ relative to $(0,h)$ is not defined.*

## 3.2 Resulting analysis of some illustrations

As already mentioned, our illustrations were initially intended to help us predict in which cases shape preservation was maintained up to the allowed limit $\min\big(\widetilde{\ell}_n,\widetilde{\ell}^{\star}_{n+2}\big)^-$. Therefore we have put emphasis on pointing out the non-shape preservation rather that on the exact behaviour of the final control polygon when reaching this limit. Through the existing illustrations, we will nevertheless show what we can visually learn about the critical lengths for design.

With this in view, let us return to our basic example "polynomial spaces included in cycloidal spaces", illustrated in Figure 2. Given initial control points $P_0,\dots,P_n$, all final control points $P^{\star}_1,\dots,P^{\star}_{n-1}$ visually seem to behave in a reasonable way, except for

- the central one if $n=2k$, that is, $P^{\star}_{k+1}$;

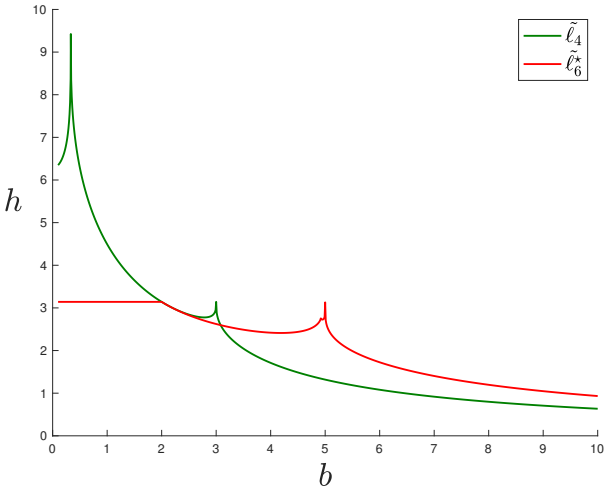


Figure 13: Left: $\widetilde{\ell}_4(b)$ for $p_4(x) = x(x^2+1)(x^2+b^2)$ (green curve) and $\widetilde{\ell}_6^\star(b)$ for $p_6^\star(x) = p_4(x)(x^2+9)$ (red curve), see (10).

- the central two ones if $n = 2k+1$, that is, $P_{k+1}^\star$, $P_{k+2}^\star$,

these points visibly going to infinity as $h$ reaches $\widetilde{\ell}_{n+2}^{\star -}$, this being obvious through additional pictures closer to the limit which are not shown here. According to the various statements in the previous subsection, we obtain visual evidence of the following result which provides a tangible geometric interpretation of the results on critical lengths of cycloidal spaces in [5, 6], see Section 3.3 below.

**Theorem 3.4.** *For $n \geqslant 2$, the critical length for design $\widetilde{\ell}_{n+2}^\star$ of the cycloidal space $\mathbb{E}_{n+2}^\star$ is the smallest positive $h$ at which the central (two) Bézier point(s) do(es) not exist – or is (are) at infinity –, while all others do exist. Equivalently, it is the smallest positive value of $h$ for which $\Delta_i^\star(0,h) = 0$ for $i = \lfloor \frac{n+1}{2} \rfloor$ and only for this integer $i \geqslant (n+1)/2$.*

In all other symmetric examples considered in Section 2, the space $\mathbb{E}_{n+2}^\star$ depends on a positive parameter $b$ in function of which we obtained the graph of $\widetilde{\ell}_{n+2}^\star = \widetilde{\ell}_{n+2}^\star(b)$ as a function of $b$, determined via the numerical procedure in [3]. In general this graph is composed of several smooth parts joining by cusps. Given a situation $\mathbb{E}_n \subset \mathbb{E}_{n+2}^\star$, on a given interval for which we have $\widetilde{\ell}_n > \widetilde{\ell}_{n+2}^\star(b)$, we can approach $\widetilde{\ell}_{n+2}^\star(b)^-$ within the segment $]\widetilde{\ell}_n, \widetilde{\ell}_{n+2}^\star(b)[$, and we can therefore visually conclude which Bézier point(s) do(es) not exist at $\widetilde{\ell}_{n+2}^\star$. From this point of view, the example in Figure 10, left, will be our reference example. Since $n = 4$ we only have to read the possible non-existence of the Bézier points $\Pi_i^\star(0,h)$, $i = 3,4,5$, of a mother-function in $\mathbb{E}_{n+2}^\star$ on the corresponding points $P_i^\star(0,h)$, $i = 3,4,5$, of the final control polygon. However we can do that only in the intervals where $\widetilde{\ell}_4 > \widetilde{\ell}_6^\star(b)$, that is, only for $b \in ]2, +\infty[\setminus\{5\}$. The rightmost pictures in Figure 11 do not provide a convincing answer, as could be the case if we had gone closer to $\widetilde{\ell}_{n+2}^\star(b)^-$.

We cannot derive similar conclusions for $b \in ]0,2]$ since, on that interval, we have $\widetilde{\ell}_6^\star(b) > \widetilde{\ell}_4$. This is why, in order to know which among the points $\Pi_i^\star(0,h)$, $i = 3,4,5$, do not exist for $h = \widetilde{\ell}_6^\star(b)$, we change the initial space $\mathbb{E}_4$, now working with

$$p_4(x) = x(x^2+1)(x^2+b^2), \quad p_6^\star(x) = p_4(x)(x^2+9). \tag{10}$$

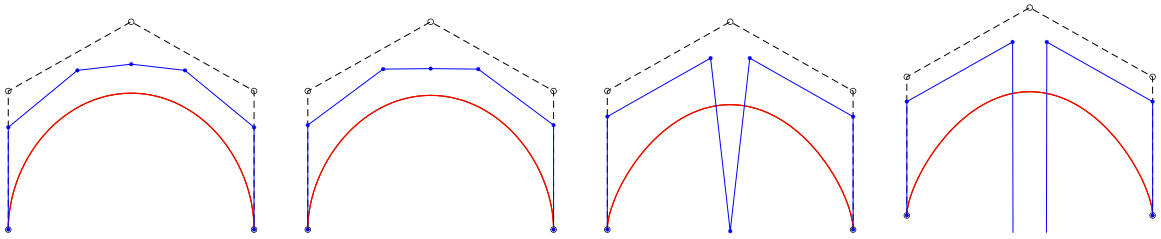

(a) $h = 2.2$ (b) $h = 2.4$ (c) $h = 3.07$ (d) $h = 3.14$

Figure 14: Dimension elevation procedure corresponding to (10) for $b = 1.5$

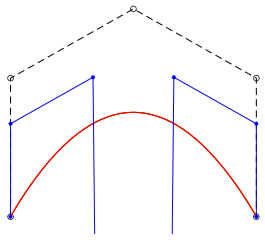

Figure 15: Dimension elevation procedure corresponding to (10), with, $b = 1.99$ and $h = 3.14$.

Figure 13 represents again the graph of $\widetilde{\ell}_6^\star(b)$ (red curve) along with the graph of $\widetilde{\ell}_4^\star(b)$ (green curve). In this new situation, we actually have

$$\widetilde{\ell}_4^\star(b) > \widetilde{\ell}_6^\star(b) \quad \text{for} \quad b \in ]0, 3[\setminus\{2\}.$$

In Figure 14, we illustrate the corresponding dimension elevation procedure for $b = 1.5$ and with various values of $h$. We can see that when $h$ approaches $\pi^-$, the central point $P_3^\star$ goes to infinity. We can therefore conjecture that, along the horizontal red segment $b \in ]0, 2[$, it is the point $\Pi_3^\star(0, \pi)$ which does not exist. This is clearly confirmed in Figure 15, with $b = 1.99$ and $h = 3.14$. What happens along the red curve segment $b \in ]2, b_0[$, where $b_0 < 5$ is the first of the two cusps close to each other, is illustrated in Figure 16. We can thus conjecture that on $]2, b_0[$, it is the point $\Pi_5^\star(0, \widetilde{\ell}_6^\star(b))$ which does not exist (or is at infinity). Afterwards, we can see the consistency with Figure 11, (h) and (l).

We cannot conclude anything about the existence of the Bézier points $\Pi_i(0, \widetilde{\ell}_6^\star(b))$ from the situation (10) for $b \in ]b_0, 5[$, or $b > 5$. However, concerning these segments we know that we can conclude from the previous situation (7) addressed in Figure 10, left, and Figure 11. For instance, for $b = 6$, given that $\widetilde{\ell}_6^\star(6) \approx 1.7245$, we additionally considered dimension elevation with $h = 1.72$. We could then clearly conjecture that, for $b > 5$, its is again the central point $\Pi_3^\star(0, \widetilde{\ell}_6(b))$ which is located at infinity, which is consistent with Figure 11, (p) and (t).

### 3.3 From Bézier points to Wronskians

Theorem 3.2 has provided a silmple geometric understanding of the critical length for design, in terms of the existence of the Bézier points of any given mother-function. In the same situation, we will now apply it to a specific one. Let $S \in \mathbb{E}_n$ be characterised the conditions

$$S(0) = S'(0) = \cdots = S^{(n-1)}(0) = 0, \quad S^{(n)}(0) = 1.$$

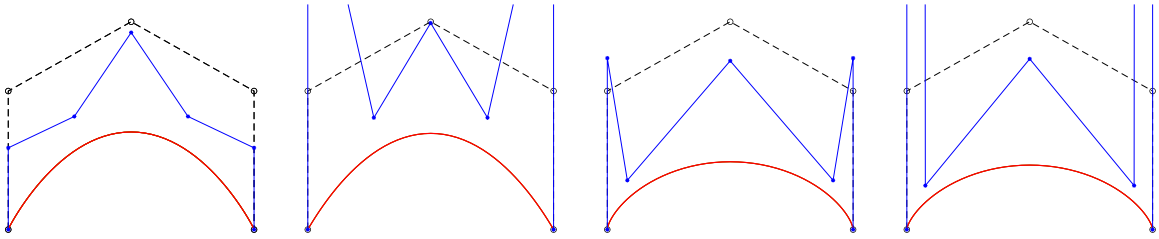

(a) $b = 2.3$, $h = 2.9$ (b) $b = 2.3$, $h = 2.936$ (c) $b = 2.95$, $h = 2.6$ (d) $b = 2.95$, $h = 2.639$

Figure 16: Dimension elevation procedure corresponding to (10), with, in (a) and (b): $(\widetilde{\ell}^{\star}_6(b), \widetilde{\ell}^{\star}_4(b)) = (2.936^+, 2.94^+)$; in (c) and (d): $(\widetilde{\ell}^{\star}_6(b), \widetilde{\ell}^{\star}_4(b)) = (2.639^+, 2.848^+)$.

Apply the previous statements to the mother-function

$$\Phi := \left(S, S', \dots, S^{(n-1)}\right).$$

Then, we clearly have:

$$\Delta_i(0, h) = \pm\, W\left(S', S'', \dots, S^{(n-i)}\right)(h), \quad h > 0, \quad 1 \leqslant i \leqslant n-1,$$

The following characterisation readily follows:

**Corollary 3.5.** *With the same data as in Theorem 3.2, the critical length for design $\widetilde{\ell}_n$ is the minimum among the positive zeroes of all Wronskians $W\left(S', S'', \dots, S^{(k)}\right)$, $1 \leqslant k \leqslant n-1$, if any. This can be reduced to all Wronskians $W\left(S', S'', \dots, S^{(k)}\right)$, $1 \leqslant k \leqslant \frac{n}{2}$, when $p_n$ is either odd or even.*

In particular, translated in terms of Wronskians, our visual Theorem 3.4 says that the critical length for design $\widetilde{\ell}^{\star}_n$ of the $(n+1)$-dimensional cycloidal space $\mathbb{E}^{\star}_n$ (which is also the critical length of the cycloidal space $\mathbb{E}^{\star}_{n-1}$) is the first positive zero of $W\left(S', \dots, S^{(k)}\right)$ whether $n = 2k$ or $n = 2k+1$. Moreover none of the other Wronskians $W\left(S', \dots, S^{(i)}\right)$, $1 \leqslant i \leqslant \frac{n}{2}$, vanishes on $]0, \widetilde{\ell}^{\star}_n]$. This corresponds to the result proved in [6] for which Theorem 3.4 provides a clear geometric understanding.

More generally, in each of our examples depending on a positive parameter $b$, our (not complete) analysis in terms of Bézier points can be translated in terms of Wronskians to help conjecture which ones are "active" on each part of the graph of the critical length for design $\widetilde{\ell}^{\star}_{n+2}(b)$.

# 4 Conclusion

So far, on purpose to facilitate the presentation, we have considered only symmetric spaces, that is with odd/even $p_n$, and with purely imaginary roots for the degree 2 polynomial $q_2$ such that $p^{\star}_{n+2} = p_n\, q_2$. However, there is no problem performing the same with non-symetric spaces. We illustrate this in Figure 17, with the double procedure $\mathbb{E}_2 \subset \mathbb{E}^{\star}_4 \subset \mathbb{E}^{\star\star}_6$, where $\mathbb{E}_2$ is spanned by the three functions $1, \cos x, \sin x$, $\mathbb{E}^{\star\star}_6$ by $\mathbb{E}_2$ and the four functions $e^x \cos(bx), e^x \sin(bx), e^{-x} \cos bx, e^{-x} \sin bx$, with $b > 0$. The intermediate space $\mathbb{E}^{\star}_4$ is the non-symmetric space spanned by $\mathbb{E}_2$ and the two functions $e^x \cos(bx), e^x \sin(bx)$. Sarting from a given symmetric control polygon $[P_0, P_1, P_2]$ we can

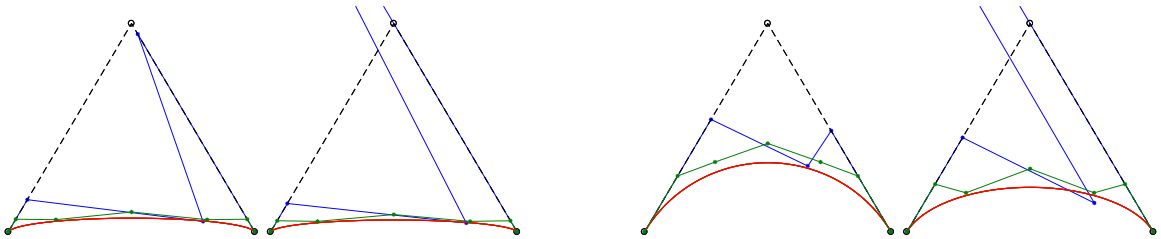

(a) $b = 1.6$, $h = 3$ (b) $b = 1.6$, $h = 3.02$ (c) $b = 2$, $h = 2.1$ (d) $b = 2$, $h = 2.59$

Figure 17: Two dimension elevation steps $\mathbb{E}_2 \subset \mathbb{E}_4^\star \subset \mathbb{E}_6^{\star\star}$, with $p_2(x) = x(x^2+1)$, $p_4^\star(x) = p_2(x)(x-1-ib)(x-1+ib)$, $p_6^{\star\star}(x) = p_4(x)(x+1-ib)(x+1+ib)$.

succesively see the blue non-symmetric control polygon $[P_0^\star, \ldots, P_4^\star]$ and finally the symmetric green control polygon $[P_0^{\star\star} \ldots, P_6^{\star\star}]$.

To permit a valuable analysis, both of the possible loss of shape preservation and of how it manisfests, we have limited our illustrations to examples of spaces depending on at most one parameter. Of course, this is very limited since the more the dimensions increase, the greater number of parameters can be involved. At the moment, we get the impression that the richness of the class of all kernels of linear differential operators with constants coefficients implies that no rule is really predictable beyond the clear fact that, in all situations such that $\widetilde{\ell}_n > \widetilde{\ell}_{n+2}^\star$, we necessarily lose shape preservation in the end.

# References


[1] R. Ait-Haddou, M-L. Mazure, H. Ruhland, A Remarkable Wronskian with Application to Critical Lengths of Cycloidal Spaces, Calcolo, 56 (45), (2019).

[2] C.V. Beccari, G. Casciola, M-L. Mazure, Piecewise Extended Chebyshev spaces: A numerical test for design, Applied Math. Comput., 296 (2017), 239–256.

[3] C.V. Beccari, G. Casciola, M-L. Mazure, Critical length: An alternative approach, J. Comp. Applied Math, 370 (2020), Article 112603.

[4] C.V. Beccari, G. Casciola, M-L. Mazure, Dimension elevation is not always corner-cutting, preprint.

[5] J.-M. Carnicer, E. Mainar, J.-M. Peña, Critical Length for Design Purposes and Extended Chebyshev Spaces, Constructive Approximation, 20 (2004), 55–71.

[6] J.-M. Carnicer, E. Mainar, J.-M. Peña, On the Critical Lengths of Cycloidal Spaces, Constr. Approx., 39 (2014), 573–583.

[7] J.-M. Carnicer, E. Mainar, J.-M. Peña, Critical lengths of cycloidal spaces are zeros of Bessel functions, Calcolo, 54 (2017), 1521–1531.

[8] M.-L. Mazure, Blossoms and optimal bases, Advances Comp. Math., 20 (2004), 177–203.

[9] M.-L. Mazure, Various characterisations of extended Chebyshev spaces, C. R. Acad. Sci. Paris, Ser. I, 339 (2004), 815–820.

[10] M.-L. Mazure, Chebyshev spaces and Bernstein bases, Constr. Approx., 22 (2005), 347–363.

[11] M.-L. Mazure, Ready-to-blossom bases in Chebyshev spaces, in *Topics in Multivariate Approximation and Interpolation*, K. Jetter, M. Buhmann, W. Haussmann, R. Schaback, et J. Stoeckler (eds), Elsevier, 12, 2006, 109–148.

[12] M.-L. Mazure, Bernstein-type operators in Chebyshev spaces, Num. Algorithms, 52 (2009), 93–128.

[13] M.-L. Mazure, Finding all systems of weight functions associated with a given Extended Chebyshev space, J. Approx. Theory, 163 (2011), 363–376.

[14] M.-L. Mazure, From Taylor interpolation to Hermite interpolation via duality, Jaén J. Approx., 4 (2012), 15–45.

[15] M.-L. Mazure, P.-J. Laurent, Nested sequences of Chebyshev spaces and shape parameters, Math. Mod.Numer. An., 32 (1998), 773–788.

[16] H. Pottmann, The geometry of Tchebycheffian splines, Comput. Aided Geom. Des., 10 (1993), 181–210.